

Metallization of the Resistivity Tensor in $\text{Bi}_2\text{Sr}_2\text{CaCu}_2\text{O}_x$ through Epitaxial Intercalation

X.-D. Xiang, W. A. Vareka, A. Zettl, J. L. Corkill, and Marvin L. Cohen

*Department of Physics, University of California at Berkeley,
and Materials Sciences Division, Lawrence Berkeley Laboratory, Berkeley, California 94720*

N. Kijima and R. Gronsky

*Department of Materials Science and Mineral Engineering, University of California,
and National Center for Electron Microscopy, Materials Sciences Division, Lawrence Berkeley Laboratory,
Berkeley, California 94720*

(Received 13 August 1991)

We have used iodine intercalation to alter the interplane interaction and the anisotropic resistivity tensor of the oxide superconductor $\text{Bi}_2\text{Sr}_2\text{CaCu}_2\text{O}_x$. Real-space transmission electron microscopy images confirm that iodine is epitaxially intercalated between the Bi-O bilayers. In the normal state above T_c , the metallic CuO_2 plane sheet resistance is unaffected by intercalation, while the out-of-plane conduction is dramatically changed from semiconductorlike to metalliclike. This result is inconsistent with some of the theoretical predictions based on holon-spinon scattering.

PACS numbers: 74.70.Jm, 74.70.Vy, 74.65.+n

The unusual normal-state properties of high- T_c copper oxides have been the focus of many theoretical studies. It has been claimed [1] that clarifying the nature of the normal state could be the key to understanding the mechanism of high- T_c superconductivity in these materials. Various theories [2] have been proposed which differ in their descriptions of the normal state, e.g., the conduction mechanisms between and within the CuO_2 planes and their role in high- T_c superconductivity.

A dramatic feature of copper oxide superconductors is their electrical transport anisotropy. The normal-state in-plane resistivity typically varies linearly with temperature, whereas the out-of-plane resistivity almost universally displays semiconductorlike behavior [3]. In addition, the ratio of the out-of-plane to in-plane resistivities can be as high as 10000. An important issue [4] is whether these anisotropies arise from the intrinsic nature of the CuO_2 network and are intimately related to T_c , or if they are just a consequence of the intermediate layer structure between CuO_2 planes with no direct relation to the superconductivity mechanism.

Recently it was demonstrated [5,6] that intercalation can induce well-defined structural changes in superconducting oxides. For example, in the stage-I iodine-intercalated $\text{IBi}_2\text{Sr}_2\text{CaCu}_2\text{O}_x$ (IBi-2:2:1:2) compound, the intercalated iodine atoms cause a 23% expansion of the crystal along the c axis and a suppression of the bulk superconducting transition temperature by ≈ 10 K. X-ray studies [5] suggest that the iodine intercalates between the Bi-O bilayers, thus affecting the interlayer coupling but leaving the intrinsic CuO_2 plane structure of the $\text{Bi}_2\text{Sr}_2\text{CaCu}_2\text{O}_x$ (Bi-2:2:1:2) host intact. This implies that the intercell coupling contribution to T_c in Bi-2:2:1:2 is about 10 K. Further evidence is provided by the observation [6] that there is only a 5-K reduction in T_c for stage-II iodine-intercalated Bi-2:2:1:2 , in which iodine

atoms intercalate into every other Bi-O bilayer.

In this Letter, we confirm the structure and report the first anisotropic transport measurements for the stage-I iodine-intercalation compound IBi-2:2:1:2 . In the normal state above T_c , intercalation is found to have no effect on the CuO_2 plane sheet resistance of the host Bi-2:2:1:2 material, but it results in a "metallization" of the out-of-plane electrical conduction. Our results are directly relevant to the above issues of interplanar coupling and the superconductivity mechanism.

Single crystals of pristine Bi-2:2:1:2 were intercalated with iodine using a gas-diffusion method described earlier [5]. The typical sample dimensions were 1.5 mm \times 1.0 mm \times 0.02 mm. X-ray diffraction confirmed the stage-I structure, and magnetization measurements showed T_c to be 80 K, consistent with previous studies [5]. Careful checks were performed to verify that the ~ 10 K depression in T_c (compared to pristine Bi-2:2:1:2) was due strictly to iodine insertion (and not, say, the "anneal schedule" used during the gas-diffusion process). In addition, to verify that the crystals were uniformly intercalated, an intercalated sample was multiply cleaved and each section was examined by x-ray diffraction. The data for each section were consistent with stage-I IBi-2:2:1:2 and showed no trace of the pristine phase.

To unambiguously determine the locations of the "guest" iodine species in the intercalated structure, crystals of pristine Bi-2:2:1:2 and intercalated IBi-2:2:1:2 were ion milled and examined in the JEOL JEM ARM-1000 atomic-resolution microscope using a through-focus series of phase-contrast images [7]. This transmission-electron-microscopy (TEM) method derives sufficient contrast to directly image the heavier cations, but not the lighter oxygen atoms. Figure 1(a) shows the atomic-resolution image of pristine Bi-2:2:1:2 , viewed along the [110] direction; Fig. 1(b) shows a corresponding com-

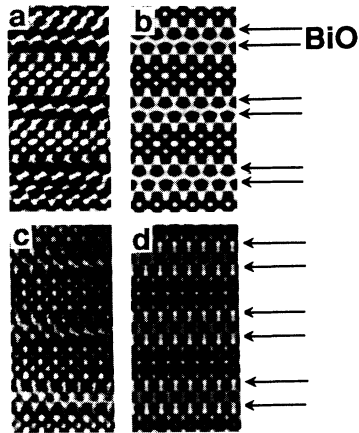


FIG. 1. Phase-contrast images of pristine and iodine-intercalated crystals. (a) Experimental micrograph of pristine Bi-2:2:1:2, (b) simulated micrograph of Bi-2:2:1:2, (c) experimental micrograph of intercalated IBi-2:2:1:2, and (d) simulated micrograph of intercalated IBi-2:2:1:2. The horizontal arrows identify Bi-O planes, between which iodine is located in the intercalated samples.

puter-generated image based on the well-known pristine Bi-2:2:1:2 structure. Note that from this viewing angle, the Bi atoms in adjacent Bi-O layers (identified by horizontal arrows) are staggered. Figure 1(c) is the atomic-resolution image of IBi-2:2:1:2, which clearly shows an expansion of the Bi-O bilayers and the positions of the iodine atoms intercalated between the Bi-O bilayers. In addition, intercalation shifts adjacent CuO_2 -plane-containing blocks into common registry, thereby removing the staggered Bi sequence observed in pristine Bi-2:2:1:2. Comparison between images recorded under [010] and [100] directions demonstrates that the iodine is located between the oxygen atoms in the sandwiching layers; therefore, the iodine is epitaxially intercalated. Although only a few atomic layers are shown in Fig. 1(c), the actual micrographs cover much larger areas ($> 1000 \text{ \AA}$), and confirm that long-range iodine order persists, consistent with x-ray studies. Figure 1(d) shows a computer-generated image [corresponding to Fig. 1(c)] assuming epitaxial iodine intercalation with a 23% c -axis expansion (3.6 \AA per Bi-O bilayer), and a shift into common registry of adjacent CuO_2 -containing blocks. Both x-ray and electron-microscopy results suggest that iodine intercalation has little effect on the internal structure of the pristine "blocks" that contain the CuO_2 planes.

The anisotropic electrical resistivity ρ was measured using standard four-terminal methods [8] (employing silver or platinum paint contacts) and a contactless rf technique [9]. In the contactless rf technique, the sample was placed between two small coaxial coils, where one coil launched a 50-MHz signal and the other coil detected the signal transmitted through the sample. The transmission amplitude was then used to determine the

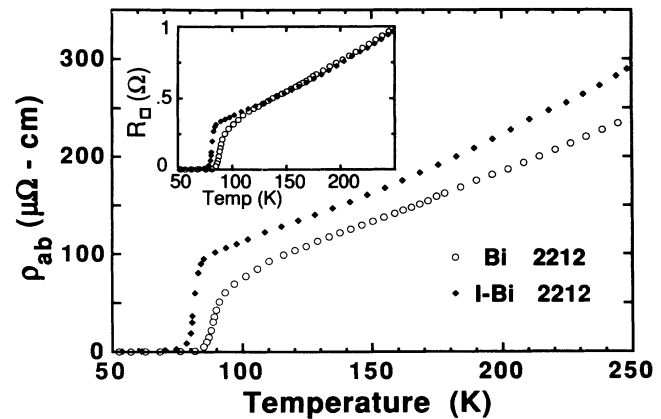


FIG. 2. In-plane resistivity for the same crystal before (Bi-2:2:1:2) and after (IBi-2:2:1:2) intercalation. Inset: The crystal sheet resistance R_{\square} before and after intercalation.

ab -plane sheet resistance of the crystal. The contactless technique has the advantage that it measures true bulk sheet resistance without being sensitive to surface conditions or contact geometries; it is well suited to a precise measurement of the in-plane resistivity of the *same* crystal before and after intercalation.

Figure 2 shows the in-plane resistivity ρ_{ab} for a given crystal before (Bi-2:2:1:2) and after (IBi-2:2:1:2) iodine intercalation, obtained using the contactless rf technique. For Bi-2:2:1:2 (open circles), ρ_{ab} displays the roughly linear temperature dependence in the normal state above T_c , as observed in many previous studies. For the same sample after intercalation (solid diamonds), ρ_{ab} shows a qualitatively similar behavior, except that, compared to pristine Bi-2:2:1:2, the magnitude of ρ_{ab} is slightly larger and T_c is somewhat depressed (consistent with magnetization studies). There also appears to be a slight change in slope in ρ_{ab} for IBi-2:2:1:2 near $T \sim 180 \text{ K}$.

Since intercalation expands the c axis of Bi-2:2:1:2 by 23%, an increase in ρ_{ab} upon intercalation is expected even in the absence of any change in the conduction properties of the CuO_2 planes (these planes are assumed to dominate the in-plane conduction). The inset to Fig. 2 shows for the same crystal the in-plane sample resistance (i.e., crystal sheet resistance, R_{\square}) before and after intercalation. Over much of the normal-state temperature range, R_{\square} is nearly identical for Bi-2:2:1:2 and IBi-2:2:1:2. Careful checks indicate that the magnitudes of R_{\square} for Bi-2:2:1:2 and IBi-2:2:1:2 agree to within 1% at room temperature (we note that possible errors in measurement of the sample thickness do not affect this result, since this dimension does not enter the analysis for R_{\square} in the contactless resistance technique). We thus conclude that the difference in ab -plane resistivity between Bi-2:2:1:2 and IBi-2:2:1:2 is a consequence only of the crystal expansion; *conduction along the CuO_2 planes is virtually unaffected by the intercalation.* On the other hand,

as we show below, intercalation dramatically changes the out-of-plane conduction.

Figure 3 shows the c -axis resistivity ρ_c as a function of temperature for a pristine Bi-2:2:1:2 crystal and an iodine intercalated IBi-2:2:1:2 crystal. Numerous pristine and intercalated specimens were measured using both the Montgomery contact geometry [8] and a large-area current and small-area voltage pad geometry with similar results. For pristine Bi-2:2:1:2 (open circles), ρ_c shows the "semiconductorlike" temperature dependence characteristic of out-of-plane transport for this and related materials. Although the increase in ρ_c with decreasing temperature has a complicated temperature dependence, it is often referred to as "1/ T -like." The solid diamonds in Fig. 3 are for IBi-2:2:1:2. In sharp contrast to the semiconductorlike temperature dependence observed in the pristine material, ρ_c for the intercalated crystal shows an absolutely linear temperature dependence over the entire normal-state range. Given that ρ_{ab} is not changed by intercalation and that TEM, electron diffraction, and visual inspection do not show any intercalation-induced defects which could couple the ab -plane into the c -axis measurement, we conclude that this temperature dependence in ρ_c is intrinsic and not due to a "tortuous path" conduction as may occur in intercalated graphite [10]. Hence, intercalation changes the semiconductorlike or 1/ T -like behavior for ρ_c into metalliclike.

Although the temperature dependence of the resistivity tensor in IBi-2:2:1:2 is metalliclike for both in-plane and out-of-plane transport, it is important to note that the in-plane to out-of-plane conduction anisotropy remains extreme. Indeed, as Fig. 3 demonstrates, the rough order of magnitude of ρ_c well above T_c is quite comparable for pristine and intercalated specimens.

There have been several predictions of the normal- and superconducting-state behavior of the layered oxides by Wheatley, Hsu, and Anderson (WHA) [11,12] and by Anderson and Zou (AZ) [13], all based on a model derived from the resonating-valence-bond theory. The ex-

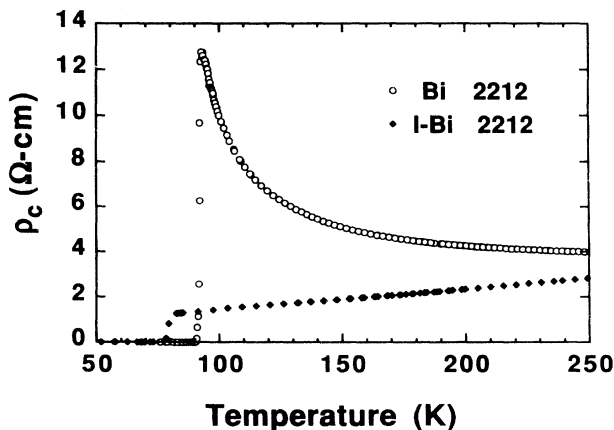


FIG. 3. Out-of-plane resistivity vs temperature for typical pristine (Bi-2:2:1:2) and intercalated (IBi-2:2:1:2) crystals.

perimental studies presented here can be used to examine these predictions and to provide information about microscopic interactions in these systems. Any viable model must account for both the small shift in T_c and the dramatic change in out-of-plane conduction induced by intercalation.

The observed change in T_c with intercalation is consistent with the WHA model of layered systems [11] if we assume that the next-nearest CuO_2 plane coupling (Λ_o) is essentially eliminated by iodine intercalation while the nearest-plane coupling (Λ_m) in the intercalated material is the same as in the pristine material since these planes are within a single block. The couplings Λ have the form

$$\Lambda_{o,m} \sim |T_{\perp o,m}|^2/J, \quad (1)$$

where $|T_{\perp}|$ is the interlayer hopping matrix element for nearest-neighbor CuO_2 planes (m) and next-nearest-neighbor planes (o), and J is the spinon bandwidth. If $\Lambda_o \rightarrow 0$, then either $T_{\perp o} \rightarrow 0$ or $J \rightarrow \infty$. The spinon bandwidth J depends only on the structure of the spinon energy spectrum which in turn is determined solely by the CuO_2 planes. The condition $J \rightarrow \infty$ is not physical nor is it reasonable, as will be shown in the discussion of ρ_{ab} below. Thus, we are left with the conclusion that $T_{\perp o} \rightarrow 0$, or is at least greatly reduced.

We now examine the anisotropic electrical resistivity. In the AZ calculation, the resistivity in the ab plane is caused by the scattering of holons by spinons. Thus, ρ_{ab} is a probe of the in-plane interaction and the densities of states of the spinons and holons. Specifically [13],

$$\rho_{ab} = (m_B/ne^2)(2\pi/\hbar)t^2g_s g_b T, \quad (2)$$

where m_B is the effective mass of the holons, n is the holon density, t is the in-plane scattering matrix element between holons and spinons, and g_s (g_b) is the spinon (holon) density of states. The value of ρ_{ab} for the intercalated samples demonstrates that the resistance of the CuO_2 planes is unchanged by the intercalation. Furthermore, the values of t , g_s , g_b , and J depend only on the spinon-holon local environment in the CuO_2 planes, and would remain constant unless the intercalation affected the structure of the material in those planes. The near-plane interlayer hopping matrix element ($T_{\perp m}$) also only depends on the local environment of the closest spaced CuO_2 planes. Thus, we can assume that t , J , g_s , g_b , and $T_{\perp m}$ are not affected by the intercalation. This supports the proposition that Λ_m is not altered by the intercalation, and that the observed depression in T_c is due to a reduction in Λ_o through a decrease in $|T_{\perp o}|$.

The out-of-plane resistivity ρ_c , however, poses a problem to an interpretation based on the AZ calculation. Intercalated samples display a metallic ρ_c down to T_c . The AZ calculation for ρ_c in a single-plane system, following a similar development as for ρ_{ab} , gives [13]

$$\rho_c = \left[\frac{\hbar}{2\pi e^2} \right] \left[\frac{ab}{c} \right] \left[\frac{1}{|T_{\perp}|^2 g_s g_b^2 T} \right], \quad (3)$$

where T_{\perp} is the interlayer matrix element for the scattering of spinons and holons, ab is the area of the Cu-Cu square in the ab plane, and c is the interlayer distance. Since in this interpretation Bi-2:2:1:2 should have two types of c -direction tunneling—from nearest-neighbor planes and next-nearest-neighbor planes—Eq. (3) is logically extended to give

$$\rho_c \sim 1/\alpha\Lambda_o T + 1/\beta\Lambda_m T, \quad (4)$$

where α and β include factors of the densities of states, J , and the different c -axis spacings for nearest-neighbor and next-nearest-neighbor CuO_2 planes.

In view of the T_c and ρ_{ab} measurements, if Λ_o decreases we would expect ρ_c for intercalated Bi-2:2:1:2 to have a dramatically *increased* $1/T$ -like behavior, whereas experiment shows no evidence for *any* $1/T$ -like behavior (see Fig. 3). In addition, the T_c measurements indicate [5] that $\Lambda_m \approx 9\Lambda_o$. Assuming the Λ_o term has been replaced by some other mechanism, with the appropriate temperature dependence, one would *still* expect to see a small $1/T$ contribution to the resistivity from the Λ_m term near T_c . However, this is not observed experimentally.

In light of this inconsistency, the previously proposed model does not adequately explain the resulting ρ_c of the iodine intercalated Bi-2:2:1:2 material. In this theory, the description of the c -axis conductivity mechanism and the pairing interaction for the superconducting state (i.e., T_{\perp}) are intimately related, and the small change in T_c and the large effect on ρ_c cannot be self-consistently accounted for.

This work was supported by the Director, Office of Energy Research, Office of Basic Energy Sciences, Materials Sciences Division of the U.S. Department of Energy under Contract No. DE-ACO3-76SF00098. J.L.C. and

M.L.C. were also supported by NSF Grant No. DMR88-18404. J.L.C. acknowledges support from an NSF Graduate Fellowship and M.L.C. acknowledges support from the J. S. Guggenheim Foundation.

-
- [1] P. W. Anderson and R. Schrieffer, *Phys. Today* **44**, No. 6, 54 (1991).
 - [2] *High Temperature Superconductivity*, edited by K. Bedell, D. Coffey, D. E. Meltzer, D. Pines, and R. Schrieffer (Addison-Wesley, Redwood City, CA, 1990).
 - [3] T. Ito, H. Takagi, S. Ishibashi, T. Ido, and S. Uchida, *Nature (London)* **350**, 596 (1991).
 - [4] See, for example, D. H. Lowndes, D. P. Norton, and J. D. Budai, *Phys. Rev. Lett.* **65**, 1160 (1990).
 - [5] X.-D. Xiang, S. McKernan, W. A. Vareka, A. Zettl, J. L. Corkill, T. W. Barbee, III, and M. L. Cohen, *Nature (London)* **348**, 145 (1990); X.-D. Xiang, W. A. Vareka, A. Zettl, J. L. Corkill, and M. L. Cohen, *Phys. Rev. B* **43**, 11496 (1991).
 - [6] X.-D. Xiang, A. Zettl, W. A. Vareka, J. L. Corkill, T. W. Barbee, III, M. L. Cohen, N. Kijima, and R. Gronsky, (unpublished).
 - [7] N. Kijima, R. Gronsky, X.-D. Xiang, W. A. Vareka, A. Zettl, J. L. Corkill, and M. L. Cohen (unpublished).
 - [8] H. C. Montgomery, *J. Appl. Phys.* **42**, 2971 (1971).
 - [9] T. Sakakibara, T. Goto, and N. Miura, *Rev. Sci. Instrum.* **60**, 444 (1989).
 - [10] I. L. Spain, in *The Physics of Semimetals and Narrow-Gap Semiconductors*, edited by D. L. Carter and R. T. Bate (Pergamon, New York, 1971), p. 177.
 - [11] J. M. Wheatley, T. C. Hsu, and P. W. Anderson, *Nature (London)* **333**, 121 (1988).
 - [12] J. M. Wheatley, T. C. Hsu, and P. W. Anderson, *Phys. Rev. B* **37**, 5897 (1988).
 - [13] P. W. Anderson and Z. Zou, *Phys. Rev. Lett.* **60**, 132 (1988).

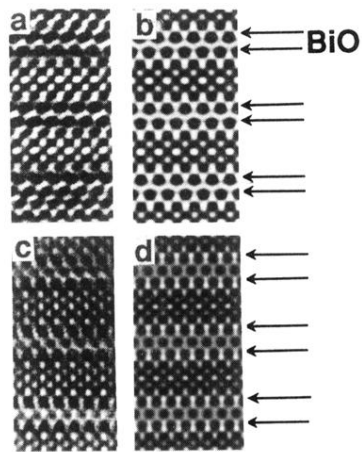


FIG. 1. Phase-contrast images of pristine and iodine-intercalated crystals. (a) Experimental micrograph of pristine Bi-2:2:1:2, (b) simulated micrograph of Bi-2:2:1:2, (c) experimental micrograph of intercalated IBi-2:2:1:2, and (d) simulated micrograph of intercalated IBi-2:2:1:2. The horizontal arrows identify Bi-O planes, between which iodine is located in the intercalated samples.